

Disturbance scaling in bidirectional vehicle platoons with different asymmetry in position and velocity coupling

Ivo Herman^a, Steffi Knorn^b and Anders Ahlén^b

^a*Department of Control Engineering, Czech Technical University in Prague, Prague, Czech Republic*

^b*Signals and Systems, Uppsala University, Sweden*

Abstract

This paper considers a string of vehicles where the local control law uses the states of the vehicle's immediate predecessor and follower. The coupling towards the preceding vehicle can be chosen different to the coupling towards the following vehicle, which is often referred to as an asymmetric bidirectional string. Further, the coupling differences, i.e., asymmetry, can be chosen differently for the velocity and the position coupling between neighbouring vehicles. This general approach includes the special cases of symmetric bidirectional strings and predecessor following control schemes. It is investigated how the effect of disturbance on the control errors in the string changes with the string length. It is shown, that in case of symmetric position coupling and asymmetric velocity coupling, linear scaling can be achieved. For symmetric interaction in both states, i.e., in symmetric bidirectional strings, the errors scale quadratically in the number of vehicles. When the coupling in position is asymmetric, exponential scaling may occur or the system might even become unstable. The paper thus gives a comprehensive overview of the achievable performance in linear, asymmetric, bidirectional platoons. The results reveal that symmetry in the position coupling and asymmetry in velocity coupling qualitatively improves the performance of the string. Extensive numerical results illustrating the theoretical findings are also presented.

Key words: Port-Hamiltonian Systems, Vehicular platoons, Multi-Vehicle Systems, Scaling, Asymmetry

1 Introduction

Vehicle platoons form an important part of future intelligent transportation systems, because such systems are anticipated to increase both the safety and capacity of highways while offering more comfort for drivers and passengers. In its simplest form, a platoon, consisting of N cooperatively-acting, automatically controlled vehicles travels in a longitudinal line with tight spacing between the vehicles.

An important safety and performance measure in this area is how the response of the platoon to disturbances scales with respect to the number of vehicles, that is, how the norm of the local errors depend on the number of vehicles N . When the local errors are bounded independently of N , the string is called “string stable”. See [21] for an overview of definitions of string stability using for instance different norms. Generally speaking, a platoon is string stable if disturbances, which are propagating through the string, do not grow with the number of vehicles or the position within the string.

Email addresses: ivo.herman@fel.cvut.cz (Ivo Herman),
steffi.knorn@signal.uu.se (Steffi Knorn),
anders.ahlen@signal.uu.se (Anders Ahlén).

The literature often distinguishes between “unidirectional” strings, where each vehicle only considers information of a group of direct predecessors, and “bidirectional”, where information from following vehicles is also used. It is well known, that a strict form of string stability in linear vehicle strings with double integrators in the open loop, local information only and tight spacing, can be achieved in neither unidirectional nor bidirectional strings [1, 22].

Bidirectional strings seem to offer advantages as more information – not only forward distance errors (towards the direct predecessor) but, additionally, backward errors (towards the direct follower) – is used to control the vehicle's motion. For example, a weaker form of string stability can be achieved [16]. In bidirectional system, the control input due to forward distance errors are often weighed as high as backward distance errors. This is referred to as a “symmetric” string. In contrast, by weighing the forward error higher, that is, allowing asymmetric controller gains, some important benefits can be obtained. The authors of [2] have shown that the approach of the eigenvalues of the formation to zero can be better when asymmetry is used. In fact, it was later proved that a uniform bound on the eigenvalues can be achieved [7, 11]. This guarantees much faster transients than what can be obtained with symmetric control.

While the eigenvalues determine the convergence speed, the transients are not solely determined by the eigenvalues. Indeed, there is a price to pay for the better convergence rate: the \mathcal{H}_∞ norm of the transfer function from the leader to the last vehicle in the platoon scales exponentially in the number of vehicles for asymmetric strings (compared to linear scaling for symmetric strings [24]). This extremely bad scaling was shown in [23] for double integrator systems and for an arbitrary agent model with two integrators in [11]. Later it was shown that the \mathcal{H}_∞ norm scales exponentially with the distance between agents [10].

Many works in the area assume that the degree of asymmetry in the position and velocity coupling is identical, see for instance [2]. However, the performance of the string can be improved by assuming symmetric position coupling and asymmetric velocity coupling. A good scaling of such an approach was numerically shown in [8] and the properties of the platoon's response to a step change in leader's velocity were derived in [5]. Using these properties, the parameters of the controller as well as the coefficient of asymmetry can be optimised to minimise the transient time [12]. In both papers [5, 12] it was shown that symmetry in position is necessary for a good scaling. In addition, it was proved in [19] that symmetry in position is a necessary condition for local string stability. Note that, when different asymmetries in velocity and position coupling are used, none of the convenient approaches presented in the literature for a distributed system analysis [6, 9] and synthesis [18, 25] can be used. The reason is that the Laplacians for position and velocity are not simultaneously diagonalisable.

Port-Hamiltonian systems analysis was used in [16] to study string stability of a bidirectional vehicle string. It was shown, that by using local drag, spring and damping terms together with integral action control, weak string stability can be guaranteed. The results were extended to analyse the effects of measurement errors in [17]. Further, using similar tools allowed the analysis of a system with a more general graph describing the inter vehicle connections instead of a simple line graph, [15].

Using the port-Hamiltonian approach for simple vehicle models in [16], this paper investigates the effect of disturbances on the norms of the state. Specifically, the paper focuses on how the norm of the response scales with the number of vehicles N for different string settings. The results are summarised graphically in Figure 1: Let h_p and h_Δ represent the asymmetry coefficients describing the asymmetry in the velocity and position coupling, respectively. Then $h_p = h_\Delta = 0$ corresponds to the symmetric, bidirectional case while $h_p = h_\Delta = 1$ describes the unidirectional ("predecessor following" = 'PF') case. For details on the system description please see Sections 3 and 4.

The contributions of this paper are as follows:

- (1) It is shown that asymmetry in velocity with symmetric position coupling, i.e., case "A" in Fig. 1, can achieve

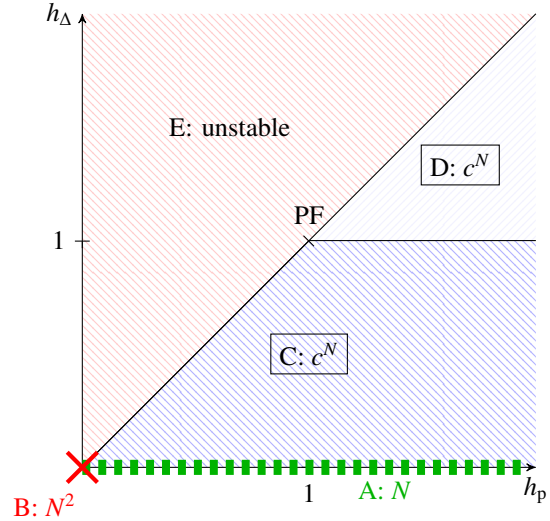


Figure 1. Scaling of a disturbance response with respect to string length N for different selections of asymmetry. Area A: linear scaling in N , Area B: quadratic in N , Area C and D: exponential in N .

linear scaling, while a completely symmetric control scales quadratically, i.e., case "B" in Fig. 1. See further Section 3.¹

- (2) It is shown that in some cases of asymmetric position coupling below a certain bound, the errors might scale exponentially, i.e., case "C" in Fig. 1, see Section 4.1. We conjecture that it is also true for $h_\Delta \geq 1$, i.e., case "D" in Fig. 1.
- (3) It is shown that for some cases of stronger asymmetry in the position coupling compared to the velocity coupling, i.e., for a subset of $h_\Delta > h_p$ of case "E" in Fig. 1, the system is unstable for a sufficiently high N , see Section 4.2. We also conjecture that for all combinations captured in case "E" a finite critical string length, which is the maximal stable string length, exists.
- (4) A comprehensive overview of the effect of asymmetry in velocity and position coupling is given. The system description unifies several existing well studied platoon descriptions such as unidirectional strings as in [22], bidirectional symmetric strings as in [1, 16] and bidirectional asymmetric strings as in [2, 5]. The results for different choices of asymmetry in velocity and position coupling include existing results for those well studied special cases. A summary and discussion of the results is found in Section 5.
- (5) Extensive numerical results are presented to illustrate the technical results, see Section 6.

Notation: The L_2 vector norm is given by $\|x\|_2 = \|x\| = \sqrt{x^T x}$ and the L_2 vector function norm by $\|x(\cdot)\|_2 = \sqrt{\int_0^\infty |x(t)|^2 dt}$.

¹ To the best knowledge of the authors, this is the first paper which analytically proves better scaling when symmetry in position and asymmetry in velocity is used. The papers [5, 12] relied in their proofs only on (reasonable, though) conjectures.

For a scalar function $H(x)$ of a vector $x = [x_1, x_2, \dots, x_n]^T$ its gradient is defined as $\nabla H(x) = \left[\frac{\partial H(x)}{\partial x_1}, \frac{\partial H(x)}{\partial x_2}, \dots, \frac{\partial H(x)}{\partial x_n} \right]^T$. The i th element of the gradient $\frac{\partial H(x)}{\partial x_i}$ is also denoted as $\nabla_{x_i} H(x)$. Denote the state and the disturbance vector by the column vectors $x(t) = \text{col}(x_1(t), \dots, x_N(t))$ and $d(t) = \text{col}(d_1(t), \dots, d_N(t))$. The column vector of ones is denoted by $\underline{1}$ and \vec{e}_i is the i th canonical vector of length N . Similarly, denote the diagonal matrix $A \in \mathbb{R}^{N \times N}$ with diagonal entries a_1, \dots, a_N as $A = \text{diag}(a_1, \dots, a_N)$. The matrix $\langle A \rangle$ is a matrix obtained from A by taking the absolute values of the elements. $A > 0$ and $A \geq 0$ denote that A is a positive definite or positive semi-definite matrix, respectively. $\sigma_i(A)$ is the i th smallest singular value of A and $\lambda_i(A)$ is the i th smallest eigenvalue. $\sigma_{\min}(A)$, $\sigma_{\max}(A)$ ($\lambda_{\min}(A)$, $\lambda_{\max}(A)$) are the minimal and maximal singular values (eigenvalues) of A , respectively.

2 System Description

Consider a system of N vehicles, modelled as double integrators. The finite mass of vehicle $i = 1, 2, \dots, N$ is denoted $m_i > 0$. The motion equations of the system can be described using the momentum and position of each vehicle, i.e., p_i and x_i , as follows

$$\dot{p}_i = F_i + d_i, \quad (1)$$

$$\dot{x}_i = m_i^{-1} p_i, \quad (2)$$

where F_i is the control force on the vehicle, d_i is the disturbance, and the momentum satisfies $p_i = m_i v_i$, where v_i is the velocity.²

In many platooning applications, the relative position between neighbouring vehicles, $\Delta_i = x_{i-1} - x_i$, is more important than the absolute position of the vehicles since controlling the inter-vehicle distances is key to avoid crashes. By collecting the positions in the vector $x(t) = \text{col}(x_1, \dots, x_N)$, and introducing $\Delta(t) = \text{col}(\Delta_1, \dots, \Delta_N)$ the local position errors can be represented by

$$\Delta(t) = -\mathcal{B}^T(x(t) - \underline{1}x_0(t)), \quad (3)$$

where the position x_0 is the reference position, i.e., the position of the virtual leader of the platoon, which the first vehicle ($i = 1$) is required to follow. The matrix \mathcal{B} describes the

² Note that this notation is often used in mechanical systems. For the description of vehicle platoons, it has also been used for instance in [16].

coupling between the vehicles and has the bidiagonal form

$$\mathcal{B} = \begin{bmatrix} 1 & -1 & 0 & \cdots & 0 \\ 0 & 1 & -1 & \ddots & \vdots \\ 0 & \ddots & \ddots & \ddots & 0 \\ \vdots & & & \ddots & 1 & -1 \\ 0 & \cdots & 0 & 0 & 0 & 1 \end{bmatrix}. \quad (4)$$

The dynamics of the string system can be described by

$$\begin{bmatrix} \dot{p} \\ \dot{\Delta} \end{bmatrix} = \begin{bmatrix} 0 & \mathcal{B} \\ -\mathcal{B}^T & 0 \end{bmatrix} \nabla H_{\text{ol}}(p) + \begin{bmatrix} F \\ 0 \end{bmatrix} + \begin{bmatrix} d \\ \vec{e}_1 v_0 \end{bmatrix}, \quad (5)$$

where $v_0 = \dot{x}_0$, $p \in \mathbb{R}^N$ is the momentum vector, i.e., $p = \text{col}(p_1, \dots, p_N)$, and the control force vector is $F = \text{col}(F_1, \dots, F_N)$. The open loop Hamiltonian function $H_{\text{ol}}(p)$ is given by

$$H_{\text{ol}}(p) = \frac{1}{2} p^T M^{-1} p. \quad (6)$$

The matrix $M \in \mathbb{R}^{N \times N}$ is the constant and positive definite inertia matrix $M = \text{diag}(m_1, \dots, m_N)$.

2.1 Symmetric Control Law

Consider the local control force F_i acting on vehicle i , to be made up by a linear combination of virtual springs (taking the position deviations towards neighbouring vehicles into account) and dampers (taking the velocity deviations towards neighbouring vehicles into account) between vehicle i and its two nearest neighbouring vehicles $i-1$ and $i+1$. This control approach is motivated by results from mechanical engineering, which studies mass-spring-damper models, and consensus algorithms for distributed second order agents.³ Since in mechanical systems it can be assumed that Newton's third law holds, that is, the forces on both sides on springs and dampers have the same magnitude, let us first introduce symmetric local damping and spring forces.

In their simplest form, the damping forces are linear and symmetric such that

$$F_i^r = \begin{cases} r_i (m_{i-1}^{-1} p_{i-1}(t) - m_i^{-1} p_i(t)) \\ \quad - r_{i+1} (m_i^{-1} p_i(t) - m_{i+1}^{-1} p_{i+1}(t)) & \text{for } 1 \leq i \leq N-1, \\ r_i (m_{i-1}^{-1} p_{i-1}(t) - m_i^{-1} p_i(t)) & \text{for } i = N, \end{cases} \quad (7)$$

³ Note that both the damping and spring forces are virtual, i.e., there are neither physical dampers, nor springs. All the coupling is realised by the onboard controller, which has at its output a control action, which causes the acceleration of the vehicle. The terms come from the fact that part of the control law is proportional to the relative velocity ("damper") and part to the distance ("spring").

where r_i describes the damping coefficient of the damper between vehicle i and its predecessor, $i - 1$. Note that, in the remainder of this paper, it is assumed that the damping coefficients are bounded from below and above:

Assumption 1 *There exist constants $\underline{r} > 0$ and $\bar{r} < \infty$ such that $\underline{r} \leq r_i \leq \bar{r}$ for all $i \leq N$.*

Hence, the vector of damping forces is described by

$$F^r = -\mathcal{B}R\mathcal{B}^T(M^{-1}p - \underline{1}v_0), \quad (8)$$

with $R = \text{diag}(r_1, \dots, r_N) > 0$ due to $r_i > 0$.

In addition to the coupling in relative velocity, assume further linear, symmetric spring forces of the form

$$F_i^s = \begin{cases} a_i(x_{i-1}(t) - x_i(t)) \\ -a_{i+1}(x_i(t) - x_{i+1}(t)) & \text{for } 1 \leq i \leq N-1, \\ a_i(x_{i-1}(t) - x_i(t)) & \text{for } i = N, \end{cases} \quad (9)$$

where $a_i > 0$ describes the spring coefficient between vehicles i and $i - 1$. Using the distance variables Δ , the vector of spring forces can be written as

$$F^s = \mathcal{B}A\Delta, \quad (10)$$

where $A = \text{diag}(a_1, a_2, \dots, a_N) > 0$.

Then, with local control $F = F^r + F^s$, the overall system can be described in the port-Hamiltonian form

$$\begin{bmatrix} \dot{p}(t) \\ \dot{\Delta}(t) \end{bmatrix} = \begin{bmatrix} -\mathcal{B}R\mathcal{B}^T & \mathcal{B} \\ -\mathcal{B}^T & 0 \end{bmatrix} \nabla H(p(t), \Delta(t)) + \begin{pmatrix} d(t) \\ 0 \end{pmatrix} \quad (11)$$

with the Hamiltonian function

$$H(p, \Delta) = \frac{1}{2}(p(t) - M\underline{1}v_0)^T M^{-1}(p(t) - M\underline{1}v_0) + \frac{1}{2}\Delta^T(t)A\Delta(t). \quad (12)$$

This Hamiltonian captures the kinetic “energy” stored in the relative velocity to the leader and potential “energy” stored in the relative distances. Since the system (11) has a symmetric coupling both in position and in velocity, it will be abbreviated SPSV (Symmetric Position, Symmetric Velocity).

Using the approach of [15], the scaling effects of the disturbance d can be analysed when the number of vehicles grows.

Theorem 2 ([15]) *Consider the system (11) with Hamiltonian (12). Then*

- (i) *the autonomous system is asymptotically stable,*
- (ii) *the system is passive with input vector $d(t)$, output vector $\nabla_p H$ and storage function (12), and*

(iii) *the following bound on the Hamiltonian at time t holds*

$$H(p(t), \Delta(t)) \leq H(p(0), \Delta(0)) + \frac{\|d(\cdot)\|_2^2}{2\sigma_{\min}(\mathcal{B}R\mathcal{B}^T)}. \quad (13)$$

Remark 3 *Note that, the influence of the disturbance onto the Hamiltonian (and hence the states) is scaled by the inverse of the smallest singular value of $\mathcal{B}R\mathcal{B}^T$. Hence, the scaling of the platoon’s disturbance response with respect to N will depend on the scaling of $\sigma_{\min}(\mathcal{B}R\mathcal{B}^T)$ with respect to N . It will be shown below that in case of asymmetric velocity coupling, the scaling depends on the minimal singular value of an altered matrix, which scales differently with respect to N , leading to a different (improved) scaling in the platoons disturbance response.*

3 Effect of Damping Asymmetry in Local Control

Assume the control input resulting from the velocity difference between two neighbouring vehicles i and $i - 1$ is weighted differently by vehicle i compared to vehicle $i - 1$. Specifically, vehicle i weighs the damping force control input of the damper between itself and its direct predecessor $i - 1$ by $1 + h_p$, whereas the damping force control input of the damper between itself and its direct follower $i + 1$ is scaled by $1 - h_p$, where $h_p > 0$ is the coefficient describing the asymmetry in the damping forces. Then, the damping force of the i th vehicle for $i < N$ is

$$F_i^r = (1 + h_p)r_i(m_{i-1}^{-1}p_{i-1}(t) - m_i^{-1}p_i(t)) - (1 - h_p)r_{i+1}(m_i^{-1}p_i(t) - m_{i+1}^{-1}p_{i+1}(t)) \quad (14)$$

and $F_N^r = (1 + h_p)r_N(m_{N-1}^{-1}p_{N-1}(t) - m_N^{-1}p_N(t))$. When discussing asymmetry in velocity coupling, the following assumption is needed:

Assumption 4 $r_i \geq r_{i+1}$ for all $i < N$.

Note that the assumption above is necessary when allowing asymmetry in velocity, i. e., $h_p > 0$, to guarantee, that (12) is still a suitable Hamiltonian function for the system. Then, the system can be described by

$$\begin{bmatrix} \dot{p}(t) \\ \dot{\Delta}(t) \end{bmatrix} = \begin{bmatrix} -(\mathcal{B} + \tilde{\mathcal{B}}_p)R\mathcal{B}^T & \mathcal{B} \\ -\mathcal{B}^T & 0 \end{bmatrix} \nabla H(p(t), \Delta(t)) + \begin{pmatrix} d(t) \\ 0 \end{pmatrix} \quad (15)$$

with the Hamiltonian function (12) and the velocity asymmetry matrix

$$\tilde{\mathcal{B}}_p = h_p \langle \mathcal{B} \rangle. \quad (16)$$

Since the system (15) has symmetric position coupling and asymmetric velocity coupling, it will be abbreviated as SPAV (Symmetric Position, Asymmetric Velocity).

A similar result as for symmetric coupling (Theorem 2), can be stated.

Theorem 5 Consider the system (15) under Assumption 4 with Hamiltonian (12). Then

- (i) the autonomous system is asymptotically stable,
- (ii) the system is passive with input vector $d(t)$, output vector $\nabla_p H$ and storage function (12), and
- (iii) the following bound on the Hamiltonian at time t holds

$$H(p(t), \Delta(t)) \leq H(p(0), \Delta(0)) + \frac{\|d(\cdot)\|_2^2}{2\sigma_{\min}((\mathcal{B} + \tilde{\mathcal{B}}_p)R\mathcal{B}^T)}. \quad (17)$$

PROOF. (i) Take H in (12) as a Lyapunov function and set $d(t) = 0$. The time derivative of H is

$$\dot{H} = \nabla^T H \begin{bmatrix} -(\mathcal{B} + \tilde{\mathcal{B}}_p)R\mathcal{B}^T & \mathcal{B} \\ -\mathcal{B}^T & 0 \end{bmatrix} \nabla H. \quad (18)$$

This yields $\dot{H} = -\nabla_p^T H (\mathcal{B} + \tilde{\mathcal{B}}_p)R\mathcal{B}^T \nabla_p H$. In order to show that $-\nabla_p^T H (\mathcal{B} + \tilde{\mathcal{B}}_p)R\mathcal{B}^T \nabla_p H < 0$, let p_i be the i th element of $\nabla_p H$. Then, since $(\mathcal{B} + \tilde{\mathcal{B}}_p)R\mathcal{B}^T$ has the tridiagonal structure (it is a graph Laplacian of the path graph)

$$\begin{bmatrix} (1+h_p)r_1 + (1-h_p)r_2 & -(1-h_p)r_2 & & & \\ & -(1+h_p)r_2 & \ddots & & \\ & & \ddots & \ddots & \\ & & & \ddots & -(1-h_p)r_N \\ & & & -(1+h_p)r_N & (1+h_p)r_N \end{bmatrix} \quad (19)$$

it follows that

$$\begin{aligned} & -\nabla_p^T H (\mathcal{B} + \tilde{\mathcal{B}}_p)R\mathcal{B}^T \nabla_p H \\ &= -(r_1(1+h_p) + r_2(1-h_p))p_1^2 + r_2(1-h_p)p_1p_2 \\ & \quad + r_2(1+h_p)p_2p_1 - (r_2(1+h_p) + r_3(1-h_p))p_2^2 + \dots \\ & \quad - r_N(1+h_p)p_N^2 \\ & \leq -r_1p_1^2 - r_2(p_1 - p_2)^2 - r_3(p_2 - p_3)^2 - \dots \\ & \quad - r_{N-1}(p_{N-1} - p_N)^2 - r_N h_p p_N^2 \\ & < 0, \end{aligned} \quad (20)$$

where Assumption 4 is used. Hence, the system is Lyapunov stable. Asymptotic stability follows using the invariance principle, see [14].

(ii) Considering $d(t)$, the derivative of the Lyapunov function (12) is $\dot{H} = -\nabla_p^T H (\mathcal{B} + \tilde{\mathcal{B}}_p)R\mathcal{B}^T \nabla_p H + \nabla_p^T H d(t)$. Taking $y = \nabla_p H$ as an output yields

$$\dot{H} \leq -\sigma_{\min}((\mathcal{B} + \tilde{\mathcal{B}}_p)R\mathcal{B}^T)|y|^2 + y^T d. \quad (21)$$

This shows that the increase in the energy of the system H is less than the ‘‘power’’ $y^T d$ applied to the system. Hence the system is passive.

(iii) Extending (21) by completing the squares leads to

$$\begin{aligned} \dot{H} & \leq -\frac{\sigma_{\min}((\mathcal{B} + \tilde{\mathcal{B}}_p)R\mathcal{B}^T)}{2}|y|^2 + \frac{|d(t)|^2}{2\sigma_{\min}((\mathcal{B} + \tilde{\mathcal{B}}_p)R\mathcal{B}^T)} \\ & \quad - \frac{\sigma_{\min}((\mathcal{B} + \tilde{\mathcal{B}}_p)R\mathcal{B}^T)}{2} \left| y - \frac{d(t)}{\sigma_{\min}((\mathcal{B} + \tilde{\mathcal{B}}_p)R\mathcal{B}^T)} \right|^2 \\ & \leq \frac{|d(t)|^2}{2\sigma_{\min}((\mathcal{B} + \tilde{\mathcal{B}}_p)R\mathcal{B}^T)}. \end{aligned} \quad (22)$$

Integrating both sides of (22) with respect to time yields the result. \square

3.1 Scaling of singular values

In both cases discussed above, that is, using symmetric velocity coupling and asymmetric velocity coupling, the effect of the disturbance depends on the minimal singular value of the damping matrices. That is,

$$H(p(t), \Delta(t)) \leq H(p(0), \Delta(0)) + \frac{\|d(\cdot)\|_2^2}{2\sigma_{\min}(L_p)} \quad (23)$$

where $L_p = \mathcal{B}R\mathcal{B}^T$ for the symmetric case (Theorem 2) and $L_p = (\mathcal{B} + \tilde{\mathcal{B}}_p)R\mathcal{B}^T$ when using asymmetry in velocity (Theorem 5). From (23), it is clear that the smaller $\sigma_{\min}(L_p)$ is, the larger the effect of the disturbance $d(t)$ will be on the total energy of the system, and therefore, also on the deviations from the equilibrium.

How the smallest singular value scales with an increasing number of vehicles for both systems will be investigated next.

Lemma 6 Consider $(\mathcal{B} + \tilde{\mathcal{B}}_p)R\mathcal{B}^T$. Then, with some constants $c_1 > 0, c_2 > 0$,

$$\sigma_{\min}((\mathcal{B} + \tilde{\mathcal{B}}_p)R\mathcal{B}^T) \geq \frac{c_1 r}{N} \quad \text{for } h_p > 0, \quad (24)$$

$$\sigma_{\min}((\mathcal{B} + \tilde{\mathcal{B}}_p)R\mathcal{B}^T) \geq \frac{c_2 r}{N^2} \quad \text{for } h_p = 0. \quad (25)$$

PROOF. See Appendix A.

Hence, the lower bound on σ_{\min} approaches zero in both cases, but the approach is slower (linear) in case of asymmetric velocity coupling, while it is quadratic in SPSV. This

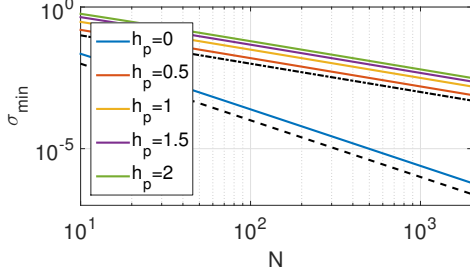


Figure 2. Scaling of $\sigma_{\min} \left((\mathcal{B} + \tilde{\mathcal{B}}_p) R \mathcal{B}^T \right)$ as a function of N and h_p for $R = I$ for $h_p = 0$ (SPSV) and increasing values of $h_p > 0$ (SPAV). The dashed and dash-dot lines are $1/N^2$ and $1/N$, respectively.

means that when asymmetric coupling in velocity is used, the effect of the disturbance is qualitatively smaller than in SPSV systems.

Lemma 6 above provides a lower bound on the scaling of σ_{\min} . The following lemma completes the picture by providing an upper bound for σ_{\min} .

Lemma 7 *The minimal singular value of $(\tilde{\mathcal{B}}_p + \mathcal{B}) R \mathcal{B}^T$ is upper bounded as follows*

$$\sigma_{\min} \left((\mathcal{B} + \tilde{\mathcal{B}}_p) R \mathcal{B}^T \right) \leq \frac{c_3 \bar{r}}{N} \quad \text{for } h_p > 0, \quad (26)$$

$$\sigma_{\min} \left((\mathcal{B} + \tilde{\mathcal{B}}_p) R \mathcal{B}^T \right) \leq \frac{c_4 \bar{r}}{N^2} \quad \text{for } h_p = 0. \quad (27)$$

with some $c_3 > 0, c_4 > 0$.

PROOF. See Appendix B.

Hence, the lower bounds (Lemma 6) and upper bounds (Lemma 7) of $\sigma_{\min} \left((\mathcal{B} + \tilde{\mathcal{B}}_p) R \mathcal{B}^T \right)$ approach zero with the same order of magnitude.

These results are also verified numerically. The scaling of the smallest singular value of the velocity coupling matrix $(\mathcal{B} + \tilde{\mathcal{B}}_p) R \mathcal{B}^T$ is shown in Fig. 2. It is clear that asymmetric coupling achieves scaling with rate $1/N$, while symmetric coupling approaches zero faster, i.e., as $1/N^2$. Note that the larger the asymmetry (greater h_p), the larger also the smallest singular value. Thus, increasing asymmetry helps in mitigating the effect of the disturbance.⁴

4 Asymmetry in position coupling

Using similar notation as in the case of asymmetric velocity coupling, define the position coupling asymmetry coefficient

⁴ Time-domain plots and scaling of other important quantities are illustrated in the Sec. 6. It confirms that in any of the quantities SPAV achieves better results.

$h_\Delta > 0$ such that the asymmetric spring forces for $i < N$ are given by

$$F_i^s = (1 + h_\Delta) a_i (x_{i-1}(t) - x_i(t)) - (1 - h_\Delta) a_{i+1} (x_i(t) - x_{i+1}(t)) \quad (28)$$

and $F_N^s = (1 + h_\Delta) a_N (q_{N-1}(t) - x_N(t))$. Also define the position coupling asymmetry matrix

$$\tilde{\mathcal{B}}_\Delta = h_\Delta \langle \mathcal{B} \rangle. \quad (29)$$

This system is abbreviated as APAV (asymmetric position, asymmetric velocity).

4.1 Asymmetry in position less than in velocity, $h_\Delta \leq h_p$

It will be shown below, that the system is stable for $h_p \geq h_\Delta$ and $h_\Delta < 1$. In contrast, it will be shown in Section 4.2, that for some cases of $h_p < h_\Delta$ the system is unstable.

In order to show stability for $h_p \geq h_\Delta$, the following scaled Hamiltonian is introduced

$$H_\Delta(p, \Delta) = \frac{1}{2} (p(t) - M \mathbf{1}_{v_0})^T E M^{-1} (p(t) - M \mathbf{1}_{v_0}) + \frac{1}{2} \Delta^T (t) (1 + h_\Delta) E A \Delta(t). \quad (30)$$

with the matrix $E = \text{diag} \left(1, \frac{1-h_\Delta}{1+h_\Delta}, \left(\frac{1-h_\Delta}{1+h_\Delta} \right)^2, \dots, \left(\frac{1-h_\Delta}{1+h_\Delta} \right)^{N-1} \right)$. This H_Δ is positive definite for $h_\Delta < 1$.

Using (30) leads to the system description

$$\begin{bmatrix} \dot{p}(t) \\ \dot{\Delta}(t) \end{bmatrix} = \begin{bmatrix} -(\mathcal{B} + \tilde{\mathcal{B}}_p) R \mathcal{B}^T E^{-1} & \frac{1}{1+h_\Delta} (\mathcal{B} + \tilde{\mathcal{B}}_\Delta) E^{-1} \\ -\mathcal{B}^T E^{-1} & 0 \end{bmatrix} \nabla H_\Delta + \begin{bmatrix} d(t) \\ 0 \end{bmatrix}. \quad (31)$$

This is a skew-symmetric form since $-(-\mathcal{B}^T E^{-1})^T = E^{-1} \mathcal{B}$ is equal to $\frac{1}{1+h_\Delta} (\mathcal{B} + \tilde{\mathcal{B}}_\Delta) E^{-1}$. To see this, rewrite the latter as $\left(\frac{1}{1+h_\Delta} \mathcal{B} + \frac{h_\Delta}{1+h_\Delta} \langle \mathcal{B} \rangle \right) E^{-1}$. It can be easily verified that $\left(\frac{1}{1+h_\Delta} \mathcal{B} + \frac{h_\Delta}{1+h_\Delta} \langle \mathcal{B} \rangle \right) = I - \frac{1-h_\Delta}{1+h_\Delta} D_u$, where D_u has ones only at the first upper-diagonal. Note also that $\frac{1-h_\Delta}{1+h_\Delta} D_u E^{-1} = E^{-1} D_u$. This yields $\left(\frac{1}{1+h_\Delta} \mathcal{B} + \frac{h_\Delta}{1+h_\Delta} \langle \mathcal{B} \rangle \right) E^{-1} = \left(I - \frac{1-h_\Delta}{1+h_\Delta} D_u \right) E^{-1} = E^{-1} - E^{-1} D_u = E^{-1} \mathcal{B}$.

Theorem 8 *Consider system (31) under Assumption 4 with Hamiltonian (30). Then,*

- (i) *the autonomous system is asymptotically stable for $h_p \geq h_\Delta$ and $h_\Delta < 1$, and*
- (ii) *the effect of disturbances is bounded as*

$$H_\Delta(t) \leq H_\Delta(0) + \frac{\|d(\cdot)\|_2^2}{2\sigma_{\min} \left(E (\mathcal{B} + \tilde{\mathcal{B}}_p) R \mathcal{B}^T \right)}, \quad (32)$$

and $\sigma_{\min}(E(\mathcal{B} + \tilde{\mathcal{B}}_p)R\mathcal{B}^T)$ approaches zero with rate $1/c^N$, with $c > 1$.

PROOF. (i) Use H_Δ in (30) as a Lyapunov function and set $d(t) = 0$. With $\tilde{v} := M^{-1}(p - M\mathbf{1}_{v_0})$ such that $\nabla_p H_\Delta = E\tilde{v}$, the time derivative is $\dot{H}_\Delta = -\tilde{v}^T E(\mathcal{B} + \tilde{\mathcal{B}}_p)R\mathcal{B}^T \tilde{v}$. This quadratic form is equivalent to the quadratic form $-\tilde{v}^T S \tilde{v}$ with $S = \frac{1}{2}(E(\mathcal{B} + \tilde{\mathcal{B}}_p)R\mathcal{B}^T + \mathcal{B}R(\mathcal{B} + \tilde{\mathcal{B}}_p)^T E)$, $S = S^T$. Thus, $-\tilde{v}^T E(\mathcal{B} + \tilde{\mathcal{B}}_p)R\mathcal{B}^T \tilde{v} < 0$ for all \tilde{v} if and only if $S > 0$. The sum s_i of the i th row of S is

$$s_i = \frac{(h_p - h_\Delta)(r_i(1 + h_\Delta) - r_{i+1}(1 - h_\Delta))(1 - h_\Delta)^{i-2}}{(1 + h_\Delta)^i} \quad (33)$$

and the sums $s_1 = \frac{(1+h_\Delta+h_p+h_\Delta h_p)r_1-r_2(h_p-h_\Delta)}{1+h_\Delta}$ and $s_N = r_N \frac{(h_p-h_\Delta)(1-h_\Delta)^{N-2}}{(1+h_\Delta)^{N-1}}$. Recall that by Assumption 4 $r_i \geq r_{i+1}$. Then if $h_p > h_\Delta$ and $h_\Delta < 1$, all sums s_i are positive, so S is positive definite. Then, the derivative \dot{H}_Δ is negative semi-definite and the invariance principle completes the proof. Stability for $h_p = h_\Delta < 1$ follows from [23, Thm 2.3].

(ii) Consider $d(t) \neq 0$. The derivative of H_Δ is $\dot{H}_\Delta = \tilde{v}^T E(\mathcal{B} + \tilde{\mathcal{B}}_p)R\mathcal{B}^T \tilde{v} + \tilde{v}^T E d$. It can be bounded since $\dot{H}_\Delta \leq -\sigma_{\min}(E(\mathcal{B} + \tilde{\mathcal{B}}_p)R\mathcal{B}^T)|\tilde{v}|^2 + \tilde{v}^T E d$. Using $L_p = (\mathcal{B} + \tilde{\mathcal{B}}_p)R\mathcal{B}^T$ and completing the squares then leads to a similar form as in (22) such that

$$\dot{H}_\Delta \leq \frac{|d|^2}{2\sigma_{\min}(E(\mathcal{B} + \tilde{\mathcal{B}}_p)R\mathcal{B}^T)}.$$

In the derivation we used the fact that $\sigma_{\max}(E) = 1$. The result (32) follows from integrating both sides with respect to time.

The smallest singular value of $E(\mathcal{B} + \tilde{\mathcal{B}}_p)R\mathcal{B}^T$ can be upper bounded as [3, Prop. 9.6.6]

$$\sigma_{\min}(E(\mathcal{B} + \tilde{\mathcal{B}}_p)R\mathcal{B}^T) \leq \sigma_{\min}(E)\sigma_{\max}((\mathcal{B} + \tilde{\mathcal{B}}_p)R\mathcal{B}^T) \quad (34)$$

The bound on $\sigma_{\max}((\mathcal{B} + \tilde{\mathcal{B}}_p)R\mathcal{B}^T)$ is $\sigma_{\max}((\mathcal{B} + \tilde{\mathcal{B}}_p)R\mathcal{B}^T) \leq \bar{r}\sigma_{\max}((\mathcal{B} + \tilde{\mathcal{B}}_p)\mathcal{B}^T) \leq 4\bar{r}$. This follows from Gershgorin Theorem applied to $((\mathcal{B} + \tilde{\mathcal{B}}_p)\mathcal{B}^T)^T(\mathcal{B} + \tilde{\mathcal{B}}_p)\mathcal{B}^T$. The smallest singular value of E is $(\frac{1-h_\Delta}{1+h_\Delta})^{N-1}$. Then,

$$\sigma_{\min}(E(\mathcal{B} + \tilde{\mathcal{B}}_p)R\mathcal{B}^T) \leq \left(\frac{1-h_\Delta}{1+h_\Delta}\right)^{N-1} 4\bar{r} \propto \frac{1}{c^N}. \quad (35)$$

with $c = \frac{1+h_\Delta}{1-h_\Delta} > 1$. Thus, $\sigma_{\min}(E(\mathcal{B} + \tilde{\mathcal{B}}_p)R\mathcal{B}^T)$ goes to zero exponentially fast. \square

Theorem 8 above means that the upper bound on the effect of the disturbance scales exponentially in the number of vehicles, which is qualitatively much worse than the scaling for symmetry in position coupling. Hence, breaking up the symmetry in position significantly deteriorates the performance.

Remark 9 *Theorem 8 above yields an upper bound. This does not mean that the system does not scale better. On the other hand, the results in the literature confirm that at least for a particular cases where $h_p = h_\Delta$ the \mathcal{H}_∞ norm of any transfer function in the formation scales exponentially with the graph distance [10]. This means that the norm of the system should scale exponentially as well. Note that similar results appeared in [11, 22, 23]. Exponential scaling can also be expected from the Lyapunov function (30), which weights the states of the vehicles exponentially towards zero with growing distance from the leader. In addition, the simulations in Sec. 6 confirm exponential scaling.*

4.2 Asymmetry in position greater than in velocity, $h_\Delta > h_p$

It will be shown below that even short strings of length $N = 2$ become unstable for particular combinations of h_p and h_Δ .

For simplicity, set $R = A = M = I$. Then, the dynamics of vehicle i for $i < N$ are given by

$$\ddot{x}_i = (1 + h_p)(v_{i-1} - v_i) + (1 - h_p)(v_{i+1} - v_i) + (1 + h_\Delta)(x_{i-1} - x_i) + (1 - h_\Delta)(x_{i+1} - x_i), \quad (36)$$

whereas the last vehicle is described by

$$\ddot{x}_N = (1 + h_p)(v_{N-1} - v_N) + (1 + h_\Delta)(x_{N-1} - x_N). \quad (37)$$

Applying the Laplace transform to both equations above and denoting $X_i = \mathcal{L}\{x_i(t)\}$, leads to the following transfer function relations

$$X_i(s) = \underbrace{\frac{(1 + h_p)s + (1 + h_\Delta)}{s^2 + 2s + 2}}_{:=G^-} X_{i-1}(s) + \underbrace{\frac{(1 - h_p)s + (1 - h_\Delta)}{s^2 + 2s + 2}}_{:=G^+} X_{i+1}(s) \quad (38)$$

$$X_N(s) = \underbrace{\frac{(1 + h_p)s + (1 + h_\Delta)}{s^2 + (1 + h_p)s + 1 + h_\Delta}}_{:=G_N} X_{N-1}(s) \quad (39)$$

Then, by writing $X_i(s) = G_i(s)X_{i-1}(s)$, the transfer functions G_i for $i < N$ can be derived recursively using the relation $G_i = (1 - G^+G_{i+1})^{-1}G^-$ such that the dynamics of the entire string can be described as illustrated in Fig. 3.

Then, it can be shown that for specific choices of h_p and h_Δ , strings of length $N = 2$ are unstable:

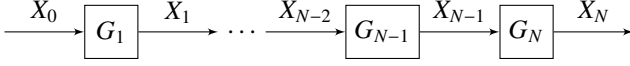


Figure 3. String model using the transfer function description $X_i(s) = G_i(s)X_{i-1}(s)$ with (38)-(39).

Lemma 10 *Strings of $N \geq 2$ vehicles are unstable if $h_\Delta \geq \frac{2h_p^4 + 12h_p^3 + 25h_p^2 + 30h_p + 11}{3h_p^2 + 6h_p + 7}$ or $h_\Delta \geq \frac{h_p^3 + 5h_p^2 + 8h_p + 10}{h_p - 1}$ for $h_p > 1$.*

PROOF. The results in (38) and (39) and tedious calculations reveal that the denominator of G_{N-1} is given by $\text{den}_{N-1} = s^4 + (3 + h_p)s^3 + (3 + h_\Delta + (1 + h_p)^2)s^2 + 2(1 + h_p)(1 + h_\Delta)s + (1 + h_\Delta)^2$. Using the Hurwitz stability criterion, it is evident that all roots of den_{N-1} have negative real parts if and only if $h_\Delta > -1$, $h_p > -3$, $h_\Delta \leq \frac{2h_p^4 + 12h_p^3 + 25h_p^2 + 30h_p + 11}{3h_p^2 + 6h_p + 7}$ and $h_\Delta \leq \frac{h_p^3 + 5h_p^2 + 8h_p + 10}{h_p - 1}$ in case $h_p > 1$. Hence, if one or more of those bounds are violated, then the second last transfer function in the string is unstable, leading to an overall unstable string. Since only nonnegative h_p and h_Δ are considered here, the bounds yield the result. \square

Similar bounds on h_Δ can also be found for the stability of the third last vehicle in the string using the same method as in the proof of Lemma 10. Fig. 4 illustrates the maximal, stable string length \bar{N}_{stab} for combinations of h_p and h_Δ . It can be seen that longer strings remain stable for smaller ratios h_Δ/h_p . Also, from Theorem 8 it follows that strings of arbitrary lengths are stable if $h_\Delta \leq h_p$ and $h_\Delta < 1$ (where the border of this region is marked with a red, solid line). Based on those observations, we formulate the following conjecture.

Conjecture 11 *For every $h_\Delta > h_p$ there exists a maximal string length \bar{N}_{stab} for which the system is stable and such that all strings of length $N > \bar{N}_{\text{stab}}$ are unstable.*

Remark 12 *Note that connecting additional vehicles to the beginning of the string leads to the additional transfer function block $G_i = (1 - G^+G_{i+1})^{-1}G^-$, which is derived recursively from the transfer function G_{i+1} . The mathematical expression reveals that this interaction is equivalent to a positive feedback loop of BIBO stable subsystems, which is known to potentially lead to closed-loop unstable systems.*

5 Discussion of the results

The results are summarised in the following theorem.

Theorem 13 *The qualitative effect of the disturbance on the energy in the system scales with the number of vehicles N as*

- (SPSV): $H(t) \leq H(0) + \|d\|_{c_1}^2 N^2$ with (12).
- (SPAV): $H(t) \leq H(0) + \|d\|_{c_2}^2 N$ with (12).

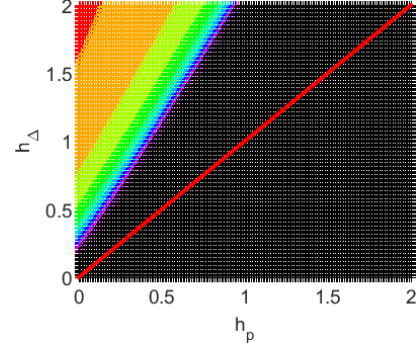


Figure 4. Maximal stable string length \bar{N}_{stab} as a function of h_p and h_Δ : $\bar{N}_{\text{stab}} = 1$ in red, $\bar{N}_{\text{stab}} = 2$ in orange, ..., $\bar{N}_{\text{stab}} = 10$ in purple, $\bar{N}_{\text{stab}} > 10$ in black

- (APAV): $H_\Delta(t) \leq H(0) + \|d\|_{c_3}^2 \frac{1}{c_3} c^N$ with (30).
This holds for $h_p \geq h_\Delta$ and $h_\Delta < 1$.

where $c_1 > 0, c_2 > 0, c_3 > 0$ and $c > 1$ are some constants independent of N . For $h_\Delta > h_p$ we conjecture instability for a sufficiently high string length N .

PROOF. The proof follows from combining Theorems 2 and 8, Theorem 5 with Lemmas 6 and 7. \square

The results of Theorem 13 are illustrated in Fig. 1. The region denoted as *A* corresponds to the case with symmetric coupling in position and asymmetric in velocity (SPAV), $h_\Delta = 0, h_p > 0$. For this, it was shown that the scaling is linear in N . When the coupling becomes symmetric also in velocity (SPSV), i.e., point *B* with $h_\Delta = 0, h_p = 0$, the scaling deteriorates to N^2 . In the region *C* the asymmetry in position is less than the asymmetry in velocity (APAV), $h_\Delta < 1$ and $h_p \geq h_\Delta$. In this region the scaling is c^N with $c > 1$, that is, exponential in the worst case (Theorem 8). We conjecture, based on numerical simulations, that the same exponential scaling occurs also in the region *D* defined as $1 \leq h_\Delta < h_p$. In the region *E*, defined as $h_\Delta > h_p$, there exist combinations of h_Δ and h_p for which even trivial strings of length $N = 2$ are unstable. We conjecture that for all $h_\Delta > h_p$ there exist a critical stable string length \bar{N}_{stab} such that the string becomes unstable for $N > \bar{N}_{\text{stab}}$.

Scaling in some of the regions were known previously. For instance, the case $h_p = h_\Delta = 1$ corresponds to the predecessor following (PF) case, for which Seiler et.al. in [22] proved that the \mathcal{H}_∞ norm grows exponentially. Later, this was generalised in [11, 23] to $0 \leq h_p = h_\Delta \leq 1$.

It is noteworthy that so far, most literature in the area of string stability has focused on case *B*, the predecessor following (PF) architecture or on identical asymmetries, that is on the line $0 \leq h_p = h_\Delta \leq 1$. However, these popular choices are clearly outperformed by case *A*, that is, choosing $h_p > 0$ and $h_\Delta = 0$. This effect is also illustrated by several numerical

simulations discussed in the following section. Therefore, we believe that the results presented in this paper should lead to a new “standard”, that is, choosing $h_p > 0$ and $h_\Delta = 0$.

5.1 Difference between springs and dampers

It is clear from Fig. 1 that whenever allowing asymmetry in the positions, i.e., $h_\Delta > 0$, the performance of the system deteriorates or the system might even become unstable. However, by introducing asymmetry only in velocity, i.e. $h_p > 0$, the scaling compared to the symmetric case is improved. This brings about the question: why are asymmetric dampers beneficial while asymmetric springs are not?

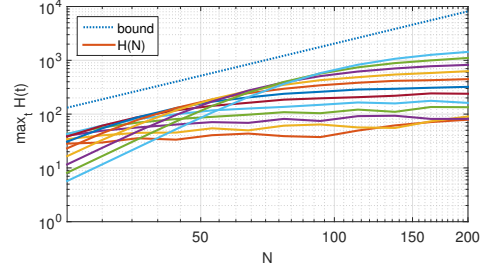
To answer this question a review of how dampers and springs process incoming energy is required. The dampers are instances of generalised resistances [13]. Hence, they only extract (“burn”) energy from the system. When introducing asymmetric dampers, only *how* the energy is extracted (dissipated) is changed.

Assume that the virtual springs between the agents are ideal. Then, by Newton’s third law (‘actio = reactio’) it should be true, that a force acting on one side of the spring is exactly the opposite of a force at the other side of the spring such that their sum is zero. However, this fundamental law is violated when introducing asymmetric springs: Consider a spring between two adjacent vehicles (preceding $i - 1$ and following i) with $A = I$ where the inter vehicle distance is bigger than desired. When introducing asymmetry, the force, which is pulling the preceding vehicle backwards, is $(1 - h_\Delta)(x_{i-1} - x_i)$, while the force, which is pulling the following vehicle forward, is $(1 + h_\Delta)(x_{i-1} - x_i)$. Together, the overall force is $-(1 - h_\Delta)(x_{i-1} - x_i) + (1 + h_\Delta)(x_{i-1} - x_i) = 2h_\Delta(x_{i-1} - x_i)$. Hence, the asymmetric, virtual spring is introducing additional forces, and hence adds energy to the system.

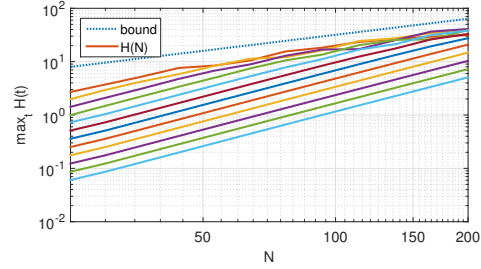
6 Examples and simulations

First, illustrative simulations confirming quadratic and linear growth are discussed. The simulation setup is the following. The input signal is $d_i(t) = \frac{p_i}{\|p\|_2 \sqrt{T_f}}$ for $t < T_f$ and $d_i(t) = 0$ for $t > T_f$. That is, the disturbance vector is parallel to the momentum vector. The time T_f is some given duration of the signal. Since the input signal has compact support, it is a proper disturbance in line with our derivations. The L_2 norm $\|d(\cdot)\|_2$ is then 1 for all N . All the simulations were started with zero initial conditions, hence $H(0) = 0$ in (12) and $H_\Delta(0) = 0$ in (30). As follows from our theorems, we are interested in the maximal value of the Hamiltonian functions $H_{\max} = \max_t H(p(t), \Delta(t))$. Note that setting the disturbance vector parallel with the momentum vector achieves the fastest growth of the energy possible, as follows from (21).

First consider SPSV. Different durations of the input signal in the range $T_f \in [200, 10000]$ were used. The plot of H_{\max}



(a) SPSV, dashed line is the quadratic bound (13)



(b) SPAV, dashed line is the linear bound (17)

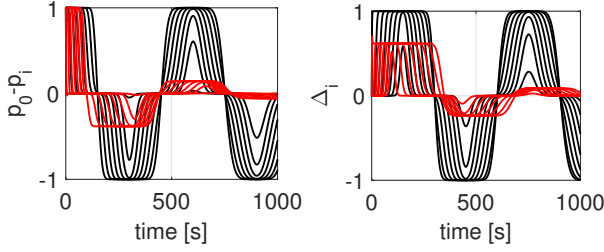
Figure 5. Plot of maximal value of $H(t)$ for SPSV (a) and SPAV (b) in logarithmic coordinates when the input is applied for different times ($T_f \in [200, 10000]$) and $N = 25, \dots, 200$.

is shown in Fig. 5a for SPSV. The solid lines correspond to different T_f . Note that, the longer the duration T_f is chosen, the lower the value for low N and the higher the maximal value of H become. On the curve for each T_f , consider the point which is the closest to the bound. From the plot in Fig. 5a it is apparent that this point scales quadratically with N . It means that the quadratic growth was achieved. The case with SPAV behaves similarly. The growth of the point, where each curve gets closest to the bound, is linear. This is illustrated in Fig. 5b. Thus, the results of Theorem 13 were verified. Note that, for a given N , $\max_t H(t)$ is much smaller for case SPAV, than for SPSV. Although the bounds are conservative, they capture the scaling qualitatively.

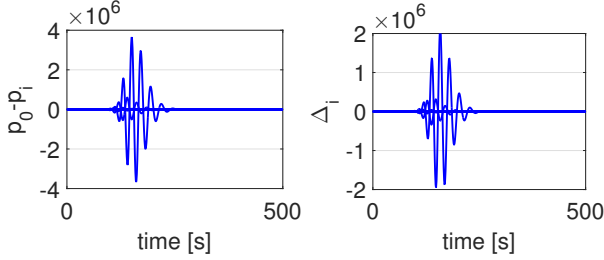
6.1 Other important characteristics

It is not only the growth of the Hamiltonian in which SPAV achieves the best scaling. Numerically, it can be shown that the SPAV control has much better transients than SPSV and APAV. As the test conditions, assume that all the initial states are zero. At time zero, the leader starts to move with unit velocity, hence its position is given as $x_0 = t$. This corresponds to an acceleration manoeuvre of the platoon. Further, it is assumed $r_i = 1, a_i = 1, m_i = 1 \forall i$, in SPAV $h_p = 0.5 \forall i$ and in APAV $h_p = 0.5, h_\Delta = 0.2, \forall i$.

When one looks at the time-domain plots in Fig. 6, it is apparent that SPAV has shorter convergence time and lower overshoots than SPSV. When asymmetry in position is introduced (APAV), extremely high peaks occur. Despite the fact that the leader moves with unit velocity, during the transient the momentum and relative positions of some vehicles



(a) Momentum SPSV, SPAV (b) Rel. positions SPSV, SPAV



(c) Momentum APAV (d) Rel. positions APAV

Figure 6. Response of the platoon with $N = 150$ to the leader's step change in velocity. Black is SPSV, red is SPAV, blue is APAV.

reached up to the order of 10^6 .

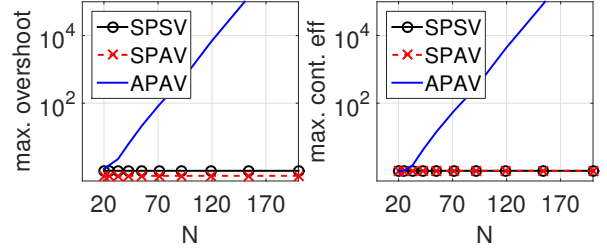
Scaling of other quantities, such as maximal overshoot, maximal control effort, convergence time and total error, is shown in Fig 7, from which the following can be observed:

- *Maximal overshoot* $\max_{i,t} \Delta_i(N,t)$ (Fig. 7a): Both SPSV and SPAV are bounded for all N , while APAV scales exponentially.
- *Maximal control effort* $\max_{i,t} F_i(t)$ (Fig. 7b): Both SPAV and SPSV have the same value equal to one, while APAV scales exponentially. The control effort of SPSV and SPAV does not grow with N .
- *Convergence time* (Fig. 7c): It is apparent that SPAV and APAV scale linearly, while SPSV scales quadratically with N . Thus, linear scaling of SPAV and quadratic scaling of SPSV appears also in the convergence time.
- *Total error* $E = \sum_{i=1}^N \int_0^{\infty} \Delta_i^2 + (v_i - v_0)^2 dt$. (Fig. 7d): Apparently, SPAV achieves the best scaling, that is, quadratic, SPSV scales cubically and APAV scales again exponentially with N .

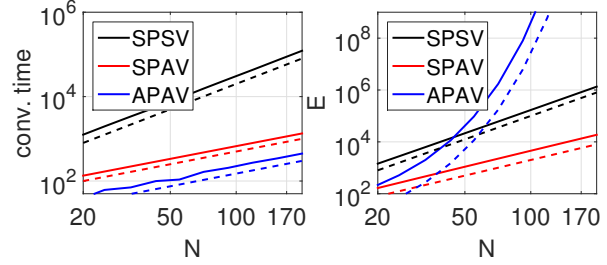
We conclude that SPAV performs the best in all cases. The only exception is the convergence time. It is true that APAV achieved about 4 times faster transient, but at the price of exponential scaling of any other quantity. We can see that SPAV has similar convergence time as APAV while keeping bounded control effort as SPSV.

7 Conclusions

This paper studied scaling in asymmetric bidirectional vehicular platoons with respect to the string length. Each ve-



(a) Max. overshoot (b) Max. cont. eff.



(c) Conv. time (d) Total error

Figure 7. Scaling of several quantities of interest as a response to the unit step in leader's velocity. Note that a) and b) are in semilogarithmic coordinates, c) and d) in logarithmic coordinates. In c) the dashed lines are $2N^2$ (black), $5N$ (red) and $1.5N$ (blue). In d) the dashed lines are $0.1N^3$ (black), $0.2N^2$ (red) and $e^{0.17N}$ (blue).

hicle was modelled as a double integrator. Different asymmetries in position and velocity were considered in order to give a complete overview of scaling depending on the type of asymmetry used.

It was shown that the effect of disturbance scales quadratically in case of symmetric coupling in position and velocity, while it scales only linearly when symmetric coupling in positions and asymmetric in velocity is considered. When allowing asymmetry also in position, exponential scaling occurs for $h_p \geq h_\Delta$ and the system becomes unstable for at least some choices of $h_p < h_\Delta$. These findings were also verified by simulations. Hence, we conclude that having symmetric coupling in position and asymmetric coupling in velocity is the best choice.

We conjecture that similar claims can be made even for different vehicle models (more realistic linear models than double integrators) and maybe also for more general graph topologies. This is a subject of our future research.

A Proof of Lemma 6

First, consider the symmetric case such that $(\mathcal{B} + \tilde{\mathcal{B}}_p)R\mathcal{B}^T = \mathcal{B}R\mathcal{B}^T$ is given by

$$\mathcal{B}R\mathcal{B}^T = \begin{bmatrix} r_1 + r_2 & -r_2 & 0 & \cdots & 0 \\ -r_2 & r_2 + r_3 & -r_3 & \ddots & \vdots \\ 0 & -r_3 & \ddots & \ddots & 0 \\ \vdots & \ddots & \ddots & r_{N-1} + r_N & -r_N \\ 0 & \cdots & 0 & -r_N & r_N \end{bmatrix}. \quad (\text{A.1})$$

Then, the minimal singular value (which is equivalent to the minimal eigenvalue in this case) can be bounded by

$$\lambda_{\min}(\mathcal{B}R\mathcal{B}^T) \geq \underline{r} \lambda_{\min} \left(\begin{bmatrix} 2 & -1 & 0 & \cdots & 0 \\ -1 & 2 & -1 & \ddots & \vdots \\ 0 & -1 & \ddots & \ddots & 0 \\ \vdots & \ddots & \ddots & 2 & -1 \\ 0 & \cdots & 0 & -1 & 1 \end{bmatrix} \right). \quad (\text{A.2})$$

Note that the matrix above is a well known matrix - a pinned Laplacian for a path graph. Its eigenvalues are given in a closed form as [20, Prop. 3.3]

$$\lambda_i = 2 \left(1 - \cos \frac{(2i-1)\pi}{2N+1} \right) = 4 \sin^2 \frac{(2i-1)\pi}{4N+2}. \quad (\text{A.3})$$

The smallest eigenvalue λ_1 can be obtained using $\sin x \approx x$ as

$$\lambda_1 = 4 \sin^2 \frac{-\pi}{4N+2} \approx 4 \left(\frac{-\pi}{4N+2} \right)^2 = \frac{4\pi^2}{16N^2 + 16N + 4}. \quad (\text{A.4})$$

It follows that the minimal eigenvalue approaches 0 with rate $1/N^2$, so

$$\lambda_{\min} \mathcal{B}R\mathcal{B}^T \geq c \underline{r} \frac{1}{N^2}, \quad c > 0. \quad (\text{A.5})$$

Now, consider the case $h_p = 1$ such that $\mathcal{B} + \tilde{\mathcal{B}}_p = \mathcal{B} + \langle \mathcal{B} \rangle = 2I$ and, hence, $(\mathcal{B} + \tilde{\mathcal{B}}_p)R\mathcal{B}^T = 2R\mathcal{B}^T$. Then, the minimal singular value of $(\mathcal{B} + \tilde{\mathcal{B}}_p)R\mathcal{B}^T$ is given by

$$\begin{aligned} \sigma_{\min} \left((\mathcal{B} + \tilde{\mathcal{B}}_p)R\mathcal{B}^T \right) &= \sqrt{\lambda_{\min}(\mathcal{B}R\mathcal{B}^T)} \\ &\geq \sqrt{\underline{r}} \sqrt{\lambda_{\min}(\mathcal{B}R\mathcal{B}^T)}. \end{aligned} \quad (\text{A.6})$$

Since it is known from above that $\lambda_{\min}(\mathcal{B}R\mathcal{B}^T)$ approaches 0 with rate $1/N^2$, it follows that for $h_p = 1$, $\sigma_{\min}((\mathcal{B} + \tilde{\mathcal{B}}_p)R\mathcal{B}^T)$ approaches zero with rate $1/N$.

To determine the decay of the smallest singular value for the case $h_p > 0$, denote $L_p = (\mathcal{B} + h_p \langle \mathcal{B} \rangle)R\mathcal{B}^T$. Then

$$\sigma_{\min}^2 \left((\mathcal{B} + h_p \langle \mathcal{B} \rangle)R\mathcal{B}^T \right) = \lambda_{\min} \left(L_p^T L_p \right)$$

The smallest eigenvalue of the matrix can be rewritten as

$$\begin{aligned} \lambda_{\min} \left(L_p^T L_p \right) &= \lambda_{\min} \left((\mathcal{B}R\mathcal{B}^T)^T (\mathcal{B}R\mathcal{B}^T) + h_p^2 \mathcal{B}R\langle \mathcal{B} \rangle^T \langle \mathcal{B} \rangle R\mathcal{B}^T \right. \\ &\quad \left. + h_p (\mathcal{B}R\langle \mathcal{B} \rangle^T \mathcal{B} + \mathcal{B}^T \langle \mathcal{B} \rangle)R\mathcal{B}^T \right) \\ &\geq \underline{r}^2 \lambda_{\min} \left(\Gamma_1 + h_p \Gamma_2 + h_p^2 \Gamma_3 \right). \end{aligned} \quad (\text{A.7})$$

with $\Gamma_1 = (\mathcal{B}R\mathcal{B}^T)^T (\mathcal{B}R\mathcal{B}^T)$, $\Gamma_2 = (\mathcal{B} \langle \mathcal{B} \rangle^T \mathcal{B} + \mathcal{B}^T \langle \mathcal{B} \rangle) \mathcal{B}^T = \text{diag}(2, 0, \dots, 0)$ and $\Gamma_3 = \mathcal{B} \langle \mathcal{B} \rangle^T \langle \mathcal{B} \rangle \mathcal{B}^T$. Restructuring leads to

$$\lambda_{\min} \left(L_p^T L_p \right) \geq \underline{r}^2 \lambda_{\min} \left(\Gamma_1 + h_p^2 \Psi_1 + h_p^2 \Psi_2 \right) \quad (\text{A.8})$$

where

$$\Psi_1 = \begin{bmatrix} 1 + \frac{2}{h_p} & 0 & -1 & 0 & 0 & 0 & 0 & \cdots & 0 \\ 0 & 2 & 0 & -1 & 0 & 0 & 0 & \cdots & 0 \\ -1 & 0 & 2 & 0 & -1 & 0 & 0 & \cdots & 0 \\ 0 & -1 & 0 & 2 & 0 & -1 & 0 & \cdots & 0 \\ \vdots & \ddots & \vdots \\ 0 & \cdots & 0 & 0 & -1 & 0 & 2 & 0 & -1 \\ 0 & \cdots & 0 & 0 & 0 & -1 & 0 & 1 & 0 \\ 0 & \cdots & 0 & 0 & 0 & 0 & -1 & 0 & 1 \end{bmatrix}, \quad (\text{A.9})$$

$$\Psi_2 = \begin{bmatrix} 0 & 0 & 0 & \cdots & 0 \\ \vdots & \vdots & \vdots & \ddots & \vdots \\ 0 & 0 & 0 & \cdots & 0 \\ 0 & \cdots & 0 & 1 & -1 \\ 0 & \cdots & 0 & -1 & 1 \end{bmatrix}. \quad (\text{A.10})$$

Using [3, Fact 5.12.2], λ_{\min} can be bounded by

$$\lambda_{\min} \left(L_p^T L_p \right) \geq \underline{r}^2 \left(\lambda_{\min} \Gamma_1 + h_p^2 \lambda_{\min}(\Psi_1) + h_p^2 \lambda_{\min}(\Psi_2) \right). \quad (\text{A.11})$$

By previous development, the smallest eigenvalue of $\Gamma_1 = (\mathcal{B}R\mathcal{B}^T)^T (\mathcal{B}R\mathcal{B}^T)$ decays with rate $1/N^4$. The matrix Ψ_2 is positive semi-definite matrix, hence $\lambda_{\min}(\Psi_2) = 0$. It remains to investigate $\lambda_{\min}(\Psi_1)$. Note that Ψ_1 is a reducible matrix. Using the permutation matrix $P = [\vec{e}_1, \vec{e}_3, \dots, \vec{e}_{N-1}, \vec{e}_2, \vec{e}_4, \dots, \vec{e}_N]$, leads to

$$\lambda_{\min}(\Psi_1) = \lambda_{\min} \left(P^{-1} \Psi_1 P \right) = \lambda_{\min} \left(\begin{bmatrix} L_1 & 0 \\ 0 & L_2 \end{bmatrix} \right), \quad (\text{A.12})$$

which is a block diagonal matrix with matrices defined as $L_1 = \tilde{\mathcal{B}}D\tilde{\mathcal{B}}^T \in \mathbb{R}^{N/2 \times N/2}$ and $L_2 = \mathcal{B}\tilde{\mathcal{B}}^T \in \mathbb{R}^{N/2 \times N/2}$ with $D = \text{diag}(1/h_p, 1, \dots, 1)$ and $\tilde{\mathcal{B}}$ has the same structure as \mathcal{B} but half the size. It follows that $\lambda_{\min}(\Psi_1) = \min\{\lambda_{\min}(L_1), \lambda_{\min}(L_2)\}$. Let $\gamma = \min\{1/h_p, 1\}$. The eigenvalues of individual matrices are given as $\lambda_{\min}(L_1) \geq \gamma\lambda_{\min}(\tilde{\mathcal{B}}\tilde{\mathcal{B}}^T)$ and $\lambda_{\min}(L_2) = \lambda_{\min}(\tilde{\mathcal{B}}\tilde{\mathcal{B}}^T)$. Hence, $\lambda_{\min}(\Psi_1) \geq \gamma\lambda_{\min}(\tilde{\mathcal{B}}\tilde{\mathcal{B}}^T)$ and

$$\lambda_{\min}(L_p^T L_p) \geq \gamma^2 (h_p^2 \lambda_{\min}(\tilde{\mathcal{B}}\tilde{\mathcal{B}}^T)). \quad (\text{A.13})$$

From (A.5) it is known that the smallest eigenvalue of $\tilde{\mathcal{B}}\tilde{\mathcal{B}}^T$ approaches zero with quadratic rate. Hence,

$$\sigma_{\min}((\mathcal{B} + h_p \langle \mathcal{B} \rangle)R\mathcal{B}^T) = \sqrt{\lambda_{\min}(L_p^T L_p)} \geq c \frac{1}{N}, \quad c > 0. \quad (\text{A.14})$$

B Proof of Lemma 7

First note that $\sigma_{\min}((\mathcal{B} + \tilde{\mathcal{B}}_p)R\mathcal{B}^T) \leq \bar{r}\sigma_{\min}((\mathcal{B} + \tilde{\mathcal{B}}_p)\mathcal{B}^T)$. Hence, it suffices to analyse $\sigma_{\min}((\mathcal{B} + \tilde{\mathcal{B}}_p)\mathcal{B}^T)$. The matrix $(\mathcal{B} + \tilde{\mathcal{B}}_p)\mathcal{B}^T$ has a form

$$(\mathcal{B} + \tilde{\mathcal{B}}_p)\mathcal{B}^T = \begin{bmatrix} 2 & -(1-h_p) & 0 & \dots & 0 \\ -(1+h_p) & 2 & -(1-h_p) & \dots & 0 \\ \vdots & \vdots & \vdots & \ddots & \vdots \\ 0 & \dots & -(1+h_p) & 2 & -(1-h_p) \\ 0 & \dots & 0 & -(1+h_p) & 1+h_p \end{bmatrix}. \quad (\text{B.1})$$

As its leading principal submatrix of size $N-1$, it has a finite Toeplitz matrix, denoted as M_N . The matrix M_N has as its symbol $a(t) = -(1-h_p)t^{-1} + 2 - (1+h_p)t^1$ with $t \in \mathbb{C}, |t| = 1$. The symbol is not Fredholm, because it has a zero at $t = 1$. The order α of the zero at $t = 1$ is either 1 for $h_p > 0$ or 2 for $h_p = 0$. The result [4, Thm. 9.8] specifies scaling of singular values for Toeplitz matrices as

$$\sigma_i(M_N) = \mathcal{O}\left(\frac{1}{N^\alpha}\right) \quad (\text{B.2})$$

for any fixed i with $\sigma_i \leq \sigma_{i+1}$. That is, the singular values go to zero with a rate at least given by the order of the zero of the symbol.

Since M_N is a submatrix of $(\mathcal{B} + \tilde{\mathcal{B}}_p)\mathcal{B}^T$, use the result [4, Thm. 9.7] on interlacing of the singular values for submatrices. It follows that

$$\sigma_{\min}((\mathcal{B} + \tilde{\mathcal{B}}_p)\mathcal{B}^T) \leq \sigma_3(M_N) \quad (\text{B.3})$$

From (B.2) follows that $\sigma_3(M_N) = \mathcal{O}\left(\frac{1}{N^\alpha}\right)$, hence $\sigma_3(M_N) \leq c/N^\alpha$. Thus, by (B.3) $\sigma_{\min}((\mathcal{B} + \tilde{\mathcal{B}}_p)\mathcal{B}^T) \leq c_1/N$ if $h_p > 0$ and $\sigma_{\min}((\mathcal{B} + \tilde{\mathcal{B}}_p)\mathcal{B}^T) \leq c_2/N^2$ if $h_p = 0$. \square

References

- [1] Prabir Barooah and Joao P. Hespanha. Error Amplification and Disturbance Propagation in Vehicle Strings with Decentralized Linear Control. In *Proceedings of the 44th IEEE Conference on Decision and Control*, pages 4964–4969. IEEE, 2005.
- [2] Prabir Barooah, Prashant G. Mehta, and Joao P. Hespanha. Mistuning-Based Control Design to Improve Closed-Loop Stability Margin of Vehicular Platoons. *IEEE Transactions on Automatic Control*, 54(9):2100–2113, sep 2009.
- [3] Dennis S. Bernstein. *Matrix Mathematics*. Princeton University Press, 2005.
- [4] Albrecht Böttcher and Sergei M. Grudsky. *Spectral Properties of Banded Toeplitz Matrices*. SIAM, 2005.
- [5] Carlos E Cantos and J. J. P. Veerman. Transients in the Synchronization of Oscillator Arrays. *Arxiv preprint*, arXiv:1308:1–11, 2014.
- [6] J. Alexander Fax and Richard M. Murray. Information Flow and Cooperative Control of Vehicle Formations. *IEEE Transactions on Automatic Control*, 49(9):1465–1476, sep 2004.
- [7] He Hao and Prabir Barooah. Stability and robustness of large platoons of vehicles with double-integrator models and nearest neighbor interaction. *International Journal of Robust and Nonlinear Control*, 23(8):2097–2122, 2012.
- [8] He Hao, Huibing Yin, and Zhen Kan. On the robustness of large 1-D network of double integrator agents. In *American Control Conference (ACC), 2012, Montreal, Canada*, pages 6059–6064, 2012.
- [9] Kristian Hengster-Movric and Frank L. Lewis. Cooperative Optimal Control for Multi-Agent Systems on Directed Graph Topologies. *IEEE Transactions on Automatic Control*, 59(3):769–774, mar 2014.
- [10] Ivo Herman, Dan Martinec, Zdeněk Hurák, and Michael Sebek. Scaling in bidirectional platoons with dynamic controllers and proportional asymmetry. *arXiv preprint 1410.3943*, pages 1–12, 2016.
- [11] Ivo Herman, Dan Martinec, Zdeněk Hurák, and Michael Sebek. Nonzero Bound on Fiedler Eigenvalue Causes Exponential Growth of H-Infinity Norm of Vehicular Platoon. *IEEE Transactions on Automatic Control*, 60(8):2248–2253, aug 2015.
- [12] Ivo Herman, Dan Martinec, and J.J.P. Veerman. Transients of platoons with asymmetric and different Laplacians. *Systems & Control Letters*, 91:28–35, 2016.
- [13] Dimitri Jeltsema and Jacquelin Scherpen. Multidomain modeling of nonlinear networks and systems. *IEEE Control Systems Magazine*, 29(4):28–59, aug 2009.
- [14] H. K. Khalil. *Nonlinear Systems*. Prentice Hall, third edition, 2001.
- [15] Steffi Knorn and Anders Ahlén. Deviation bounds in multi agent systems described by undirected graphs. *Automatica*, 67:205–210, May 2016.
- [16] Steffi Knorn, Alejandro Donaire, Juan C. Agüero, and Richard H. Middleton. Passivity-based control for multi-vehicle systems subject to string constraints. *Automatica*, 50(12):3224–3230, December 2014.
- [17] Steffi Knorn, Alejandro Donaire, Juan C Agüero, and Richard H Middleton. Scalability of bidirectional vehicle strings with static and dynamic measurement errors. *Automatica*, 62:208–212, December 2015.

- [18] Zhongkui Li, Zhisheng Duan, and Guanrong Chen. On Hinf and H2 performance regions of multi-agent systems. *Automatica*, 47(4):797–803, apr 2011.
- [19] Dan Martinec, Ivo Herman, and Michael Sebek. On the necessity of symmetric positional coupling for string stability. *IEEE Transactions on Control of Network Systems*, conditionally accepted, pages 1–9, 2015.
- [20] Gianfranco Parlangeli and Giuseppe Notarstefano. On the Reachability and Observability of Path and Cycle Graphs. *IEEE Transactions on Automatic Control*, 57(3):743–748, 2012.
- [21] Jeroen Ploeg, Nathan van de Wouw, and Henk Nijmeijer. Lp String Stability of Cascaded Systems: Application to Vehicle Platooning. *IEEE Transactions on Control Systems Technology*, 22(2):786–793, mar 2014.
- [22] Pete Seiler, Aniruddha Pant, and Karl Hedrick. Disturbance propagation in vehicle strings. *IEEE Transactions on Automatic Control*, 49(10):1835–1841, 2004.
- [23] Folkert M Tangerman, J. J. P. Veerman, and Borko D. Stosic. Asymmetric decentralized flocks. *IEEE Transactions on Automatic Control*, 57(11):2844–2853, 2012.
- [24] J J P. Veerman, Borko D. Stosic, and A Olvera. Spatial instabilities and size limitations of flocks. *Networks and Heterogeneous Media*, 2(4):2007, September 2007.
- [25] Hongwei Zhang, F. L. Lewis, and Abhijit Das. Optimal Design for Synchronization of Cooperative Systems: State Feedback, Observer and Output Feedback. *IEEE Transactions on Automatic Control*, 56(8):1948–1952, aug 2011.